Study on Flow and Heat Transfer Characteristics of LNG Expansion Bend

Xianfeng Huang [1], Hongyu Zhou[2], Zhiguo Zhang[1], Zhen Li[1], Yunwei Zhang[3], Jiangkai Lei[1], Yanbing Wang[2] and Xu Sun[2,*]

[1]PipeChina Beihai Liquefied Natural Gas Co.Ltd, Beihai, Guangxi, 536000, China
[2]National Engineering Research Center for Pipeline Safety, China University of Petroleum-Beijing, Beijing,102249, China
[3]PipeChina Nanshan(Shandong) Liquefied Natural Gas Co.Ltd, Yantai, Shandong, 265700, China

*Corresponding author's e-mail: xsun@cup.edu.cn

Abstract. During the operation of an LNG receiving terminal, the fluids within the feed pipes are typically low-temperature media such as nitrogen and liquefied natural gas. The pipelines frequently operate under ultra-low temperature conditions, and rapid temperature changes often lead to issues of thermal expansion and contraction, as well as thermal stress, which may subsequently result in a series of serious consequences and potential risks such as pipeline deformation, rupture, and leakage. Reducing the adverse effects of thermal expansion and contraction, thermal stress, and other factors in LNG pipelines is a critical issue that needs to be addressed during pipeline design and construction. In engineering, the installation of expansion bends is commonly used to address such issues. Their main function is to absorb pipeline deformation during expansion and contraction, thereby preventing bending deformation or cracks in the pipeline due to thermal stress, reducing pipeline damage, and ensuring the stable operation of the LNG pipeline system. Based on actual data from an LNG receiving terminal, this study constructs a three-dimensional model of the feed pipeline expansion bend and conducts numerical simulations of the flow and heat transfer processes under pre-cooling and cold retention cycling conditions. The temperature field distribution characteristics of the feed pipeline expansion bend are analyzed. The research results indicate that during the pre-cooling and cold retention cycling processes, the fluid temperature inside the pipeline exhibits a clear stratification phenomenon in the direction of gravity. When the fluid flows through the expansion bend, this stratified structure is disrupted, thereby reducing the temperature difference between the top and bottom of the pipeline to a certain extent. The research findings not only provide a theoretical basis with reference value for the practical application of LNG pipeline engineering but also offer beneficial guidance for engineering design and optimization in related fields.

Keywords: LNG pipeline; flow state; pre-cooling; temperature differences; Keep cold

W. He et al. (eds.), *Proceedings of the 2024 10th International Conference on Advances in Energy Resources and Environment Engineering (ICAESEE 2024)*, Atlantis Highlights in Engineering 36,
https://doi.org/10.2991/978-94-6463-708-3_23

1 Introduction

Liquid natural gas is natural gas liquefied at -162°C. Compared to gas, LNG takes up 625 times less volume [1], boosting transportation and storage efficiency, and meeting growing global demand. As LNG is low-temperature, sudden flow into a room-temperature pipe causes rapid thermal contraction. The pipe's bottom contacts cold LNG, while the top stays warmer, causing temperature stress. To prevent damage, thorough pre-cooling and insulation are necessary before pipe operation. Gradually cool the pipe using low-temperature steam until it reaches a safe temperature for LNG transport.

Many scholars have studied low-temperature fluid flow, phase transitions, and heat transfer in pipes. L. Castillo[2] analyzed compressors and refrigerants for pre-cooling, setting criteria for refrigerant selection. Changxu Wu[3] modeled hose temperatures, finding they depend on pre-cooling time, location, insulation, and nitrogen inflow. Yuan Kun[4, 5] investigated liquid nitrogen pre-cooling in horizontal pipes under low flow and gravity. Wang[6] modeled thermodynamic changes and pressurization in cryogenic tank discharges, showing external heat transfer has little effect, but internal wall heat transfer reduces performance. Ludwig[7] studied self-pressurization in cryogenic tanks, finding temperature stratification and phase change controlled by pressurization gas. In[8] tested a helium tank pressurization system with a heater, proving stable discharge pressure. Barsi[9] modeled liquid hydrogen tank discharges, predicting flow and pressurization accurately. Kassemi[10] simulated heat and mass transfer at the gas-liquid interface, analyzing its impact on pressurized discharge and pressure control in cryogenic tanks.

Based on previous research and combined with actual operational data from LNG receiving terminals, this paper studies and analyzes the entire process of pre-cooling and cold retention cycling in the feed expansion pipeline at LNG receiving terminals. Through numerical simulation methods, the distribution patterns of temperature fields in the expansion bend sections during pre-cooling and cold retention cycling are investigated. The study reveals that during pre-cooling and cold retention cycling, fluid temperature stratification also forms inside the pipeline along the direction of gravity. As the fluid flows through the expansion bends, this stratification is disrupted, reducing the temperature difference between the top and bottom of the pipeline to a certain extent and ensuring pipeline safety.

2 Modeling and Numerical Simulation of Expansion Bends

2.1 Numerical Modeling and Mesh Generation for Expansion Bends

Based on actual data from the LNG receiving terminal, a three-dimensional physical model of the expansion bend was constructed, as shown in Figure 1. The outer diameter of the pipeline is 1016mm, with a wall thickness of 12.7mm. The pipeline is equipped with two layers of cold insulation on its exterior, with the thickness of the inner cold insulation layer being 150mm and the outer cold insulation layer being 70mm, respectively.The pipeline is divided into three sections: the inlet straight pipe section, the expansion bend, and the outlet straight pipe section, all located within the same horizontal plane. The total length of the pipeline is approximately 65 meters, with the inlet straight pipe section being 30 meters long, the expansion bend structure, which is perpendicular to the x-direction, being 10 meters long, the pipe section parallel to the x-direction being 8 meters long, and the outlet straight pipe section being 10 meters long.

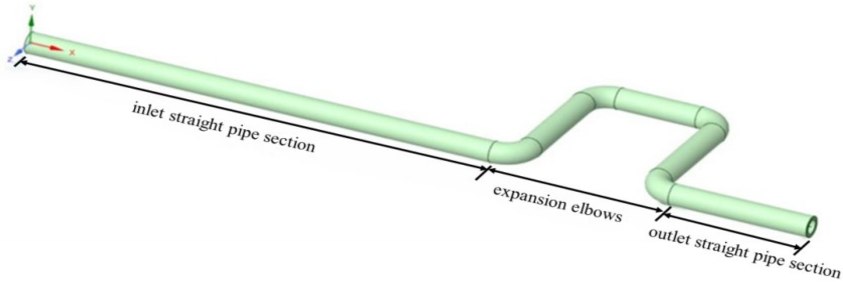

Fig. 1. D model of expansion bend pipe.

As shown in Figure 2, the model is divided using a polyhedral grid. In order to accurately simulate the flow within the boundary layer, a body-fitted grid is set up, considering both computational accuracy and computational workload. The final number of generated grids is 1.32 million, with an orthogonal quality greater than 0.5.

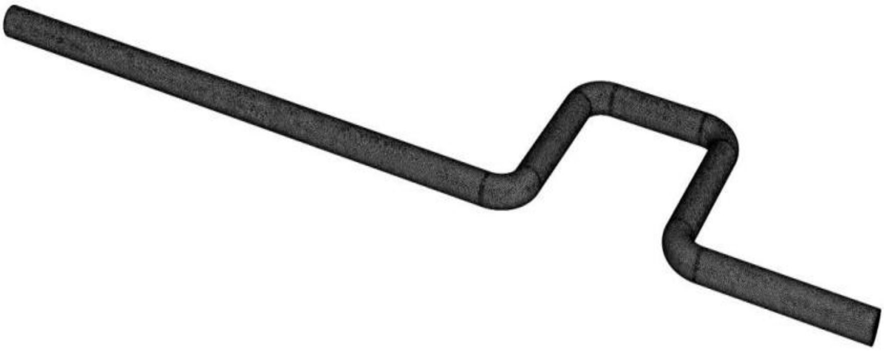

Fig. 2. Grid diagram.

As shown in Figure 3, to analyze the distribution of temperature and velocity fields within the expansion bend, a total of ten radial cross-sections are created along the flow direction of the pipeline at various pipe sections. Meanwhile, based on field conditions, temperature monitoring points qp1 and qp2, wp1 and wp2, hp1 and hp2 are established on the upper and lower wall surfaces of the pipeline at cross-sections 1, 6, and 10, respectively.

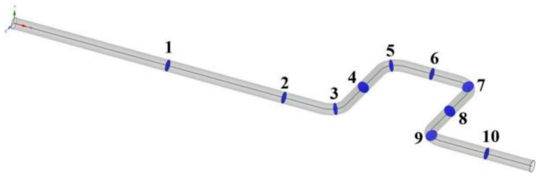

Fig. 3. Position of each radial section of the pipeline.

2.2 Numerical Simulation Method and Boundary Conditions

Based on field operational data, the pre-cooling and cold retention cycles adopt a phased injection process using low-temperature media, which takes a total of 26 hours. The fluid media utilized for the pre-cooling and cold retention cycles are low-temperature nitrogen and BOG, respectively. The pipe is made of austenitic stainless steel, with polyisocyanurate and foam glass as the inner and outer cold insulation layers, respectively.The inlet boundary conditions for the model are shown in Table 1. The pipeline flow state is turbulent, with the flow model set to the Realizable k-ε turbulence model. The boundary layer treatment selects the extended wall function. The heat transfer model includes the energy equation. Gravitational effects are considered during the flow process, with a gravitational acceleration of 9.8 m^2/s in the negative Y-axis direction. The outermost wall surface of the pipeline's cold retention layer is in direct contact with the external air, resulting in natural convective heat transfer. The convective heat transfer coefficient is set to 11.6 W/(m·K), and the ambient temperature is 303 K.

Table 1. Boundary conditions for different operating conditions.

Condition phase		Inlet temperature(k)	flow rate(m^3/h)	Pressure(Mpa)	Operating time(h)
Precooling	1	263	1000	0.2	3
	2	243	1000	0.2	3
	3	243	1500	0.2	1
	4	223	1500	0.2	3
	5	203	1500	0.2	3
	6	183	1500	0.2	2
	7	163	1500	0.2	3
	8	143	1500	0.2	3
Cold retention cycle	9	123	1500	0.2	5

2.3 Analysis of Simulation Results for Precooling and Cold Retention Cycles of Expansion Bends

The primary objective of this simulation study is to meticulously observe the flow dynamics during the precooling and cold retention cycles of the expansion bends within the LNG feed line. Special attention is given to monitoring the temperature variations across the entire bend, as well as the temperature fluctuations of the fluid within the pipeline. Comprehensive records and analyses are conducted on the temperature data obtained from the designated fluid temperature monitoring points and solid temperature monitoring points.

2.3.1. Analysis of Pipeline Wall Temperature. Figure 4 depicts the temperature distribution of the pipe wall after the completion of different pre-cooling stages. Figures a to e represent the temperature field distribution of the pipe wall at the end of the 1st stage of pre-cooling, the end of the 3rd stage of pre-cooling, the end of the 4th stage of pre-cooling, the end of the 6th stage of pre-cooling, the end of the 8th stage of pre-cooling, and the end of the cold retention cycle stage, respectively.As time progresses, the overall temperature of the pipe wall gradually decreases. At the same instant, along the flow direction in the inlet straight pipe section, the pipe wall temperature gradually increases; whereas the temperature difference between the pipe wall surfaces of the expansion bend and the outlet section is insignificant. Additionally, the circumferential distribution of the pipe wall temperature is uneven, with the temperature of the upper wall being higher than that of the lower wall, especially noticeable at the inlet straight pipe section before the expansion bend. In the expansion bend section, besides the temperature difference between the upper and lower wall surfaces, the pipe wall temperature on the outer side of the bend is lower than that on the inner side when passing through the bend.

According to the monitoring data, as the pre-cooling and cold retention cycles proceed, the temperatures at each point continue to decrease, with the temperatures at the bottom of the pipe wall being lower than those at the top at the same time. At the end of the low-temperature nitrogen pre-cooling process, the highest and lowest temperatures among the monitoring points are 176K and 148.4K, respectively. After the cold retention cycle concludes, the highest and lowest temperatures among the monitoring points are 142.2K and 128.3K, respectively, which basically meet the temperature requirements of the process. Comparing the monitoring points at the bottom of the pipe wall, the temperature at qp2 is lower than that at the other two points, wp2 and hp2, with a smaller temperature difference between wp2 and hp2. However, comparing the monitoring points at the top, the temperature at qp1 is higher than that at wp2 and hp2, which differs from the temperature distribution pattern observed in horizontal straight pipes and tank inlet pipes, where the temperature decreases as you move closer to the inlet.

Upon analyzing the temperature monitoring data specifically for the top and bottom of the pipe, it is observed that during each pre-cooling stage, the temperature difference between the top and bottom of each point first increases and then decreases. The temperature differences between the top and bottom of the pipe wall at the expansion bend (wp) and the outlet section (hp) are more similar and both are smaller than that at the inlet section (qp). The peak temperature differences between the top and bottom at qp, wp, and hp can reach 36.2 K, 21.5 K, and 24.2 K, respectively, all of which are below the 50 K required by engineering standards.

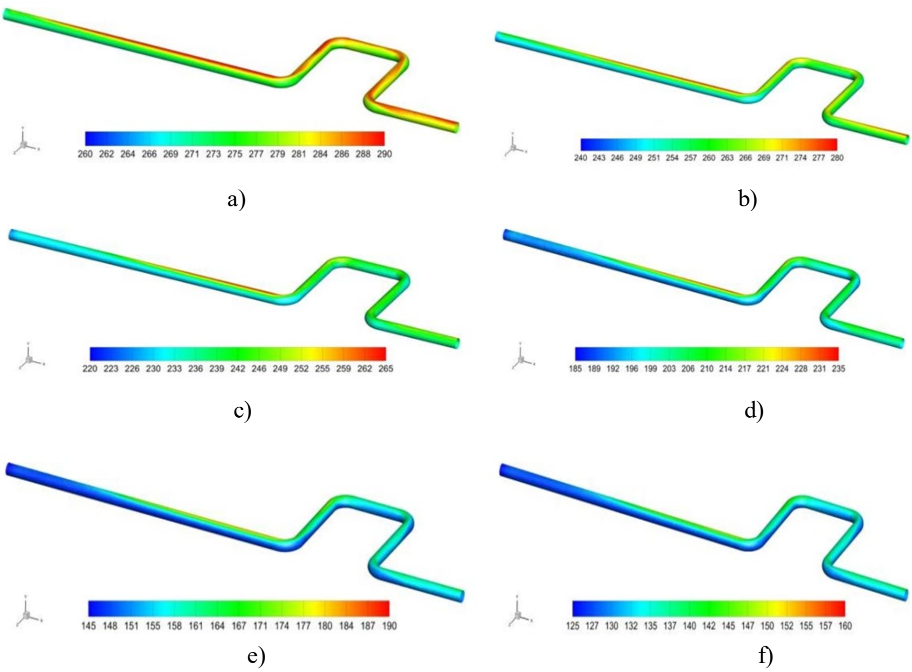

Fig. 4. Temperature distribution on the pipe wall at different times.

Figure 5 illustrates the variation of temperature decrease rate at the top of the monitoring points in the pipeline over time. As the pre-cooling boundary conditions change in stages, the temperature decrease rate at the top of each point continues to alter. Within the same pre-cooling stage, the temperature decrease rate at qp1 generally increases gradually, while it decreases gradually at hp1. Therefore, at the beginning of each stage, the temperature decrease rate follows the order qp1 < wp1 < hp1, and the order reverses at the end. Throughout the entire process, the temperature decrease rates at the top of each point are relatively low. The maximum rate at qp1 reaches 11.4 K/h at the 13th hour, while at other times, it remains basically stable below 10 K/h, which is within a relatively safe range.

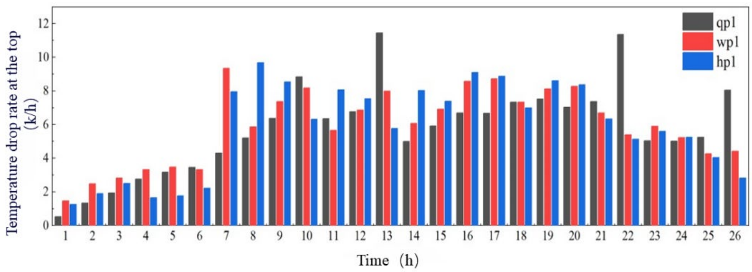

Fig. 5. The variation of temperature drop rate at the top of pipe wall over time.

Figure 6 represents the variation of temperature decrease rate at the bottom of the monitoring points in the pipeline over time. Within each pre-cooling stage, the temperature decrease rate at the bottom of each point follows a similar pattern, gradually decreasing as time progresses. Similar to the temperature decrease rate at the top, the rate at qp2 is higher than that at wp2 and hp2 at the beginning of each stage, and the order reverses at the end. Compared to the top, the temperature decrease rates at the bottom of each point fluctuate more significantly, reaching their peak at the beginning of each stage with an average exceeding 10 K/h. The maximum temperature decrease rate at qp2 reaches 14.6 K/h at the 16th hour, and then the rates decrease, remaining within a safe range overall.

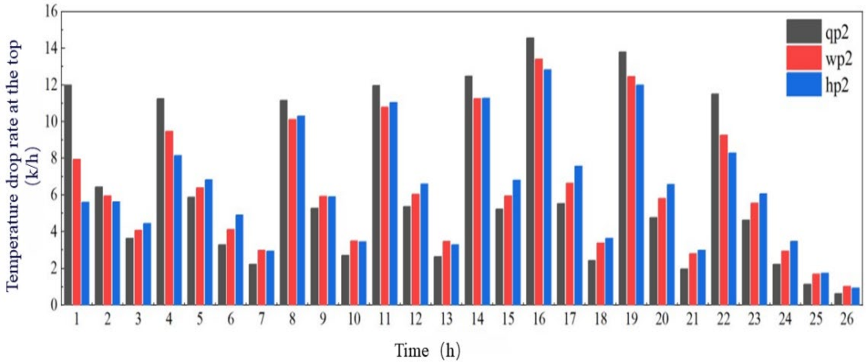

Fig. 6. The variation of temperature drop rate at the bottom of pipe wall over time.

2.3.2 Analysis of the Fluid Temperature Field Inside the Pipe. As shown in Figure 7, the fluid temperature distribution within the pipe cross-section in the horizontal direction at the end of different pre-cooling stages is depicted. Figures a to e represent the fluid temperature field distribution inside the pipe at the end of the 1st stage of pre-cooling, the end of the 3rd stage of pre-cooling, the end of the 4th stage of pre-cooling, the end of the 6th stage of pre-cooling, the end of the 8th stage of pre-cooling, and the end of the cold retention cycle stage, respectively. As pre-cooling progresses, the fluid temperature inside the pipe gradually decreases, with colder and more abundant cooling capacity fluid gradually shifting from the inlet towards the outlet section. At the same time, the fluid temperature gradually rises along the flow direction. The fluid temperature in the inlet straight pipe section drops the fastest, and by the end of the pre-cooling stage, it is closest to the injection temperature of the medium, making this section the first to complete pre-cooling. In the expansion bend section, as the fluid passes through each bend, the temperature distribution changes, with the fluid temperature on the outer side of the bend being lower than that on the inner side. This results in a similar temperature distribution in the downstream straight pipe following the bend, with a section of lower temperature. After flowing through multiple bends, this phenomenon diminishes, and the fluid temperature distribution gradually becomes more uniform.

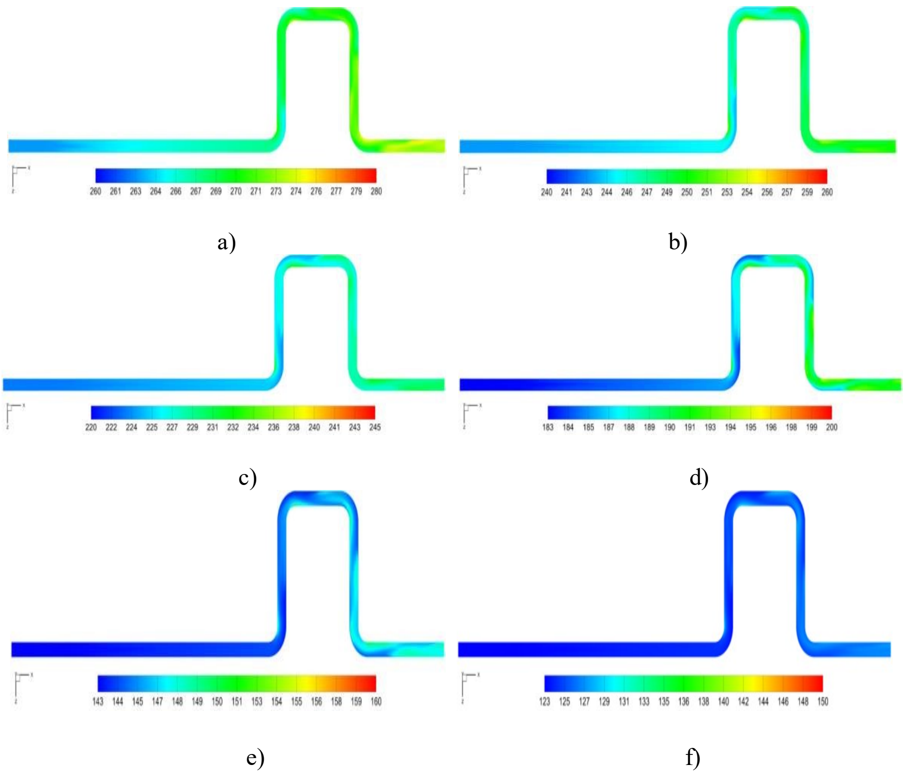

Fig. 7. Temperature distribution of fluid inside the pipe at the end of different pre cooling stages.

Taking the 4th stage of pre-cooling as an example for further analysis of the fluid temperature distribution pattern, the variation curve of fluid temperature along the pipe axis at different times during the 4th stage and the fluid temperature contour map within the expansion bend pipe after 8 hours of pre-cooling are plotted, as shown in Figures 8 and 9, respectively. From the two figures, it can be seen that the fluid temperature overall shows an upward trend along the axis. At the expansion bend, there are fluctuations in the fluid temperature. Due to the disturbance caused by the bend, low-temperature fluid accumulates on the outer side of the bend and the corresponding side of the straight pipe section. Therefore, the fluid temperature in the straight pipe section after passing through the bend experiences a slight decrease and then rises again. As pre-cooling progresses, these fluctuations gradually weaken.

Figure 10 shows the temperature distribution along the axial cross-section of the pipe in the direction of gravity every hour during the 4th stage. The fluid temperature continuously rises along the flow direction. Due to the influence of gravity and buoyancy, temperature stratification occurs in the fluid within each pipe segment in the direction of gravity. After each bend, the temperature stratification is disturbed. Therefore, after flowing through the expansion bend, the temperature stratification in the fluid of the outlet straight pipe segment is blurrier compared to the inlet segment, and the temperature distribution becomes more uniform.

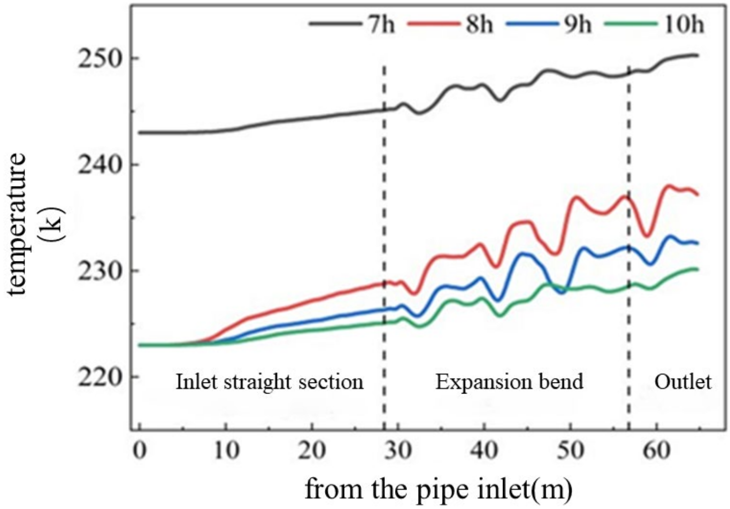

Fig. 8. Axial fluid temperature of pipelines at different times.

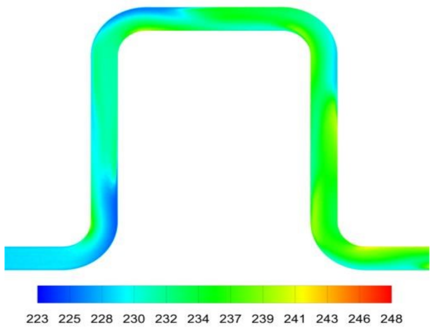

Fig. 9. Temperature distribution of fluid in expansion bend pipe after 8 hours cooling.

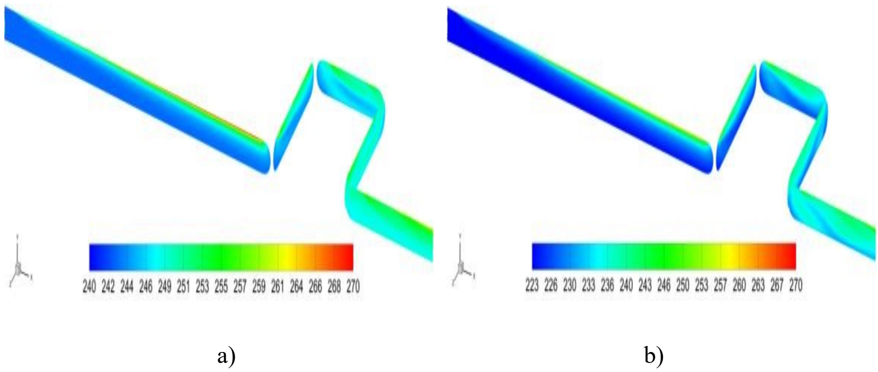

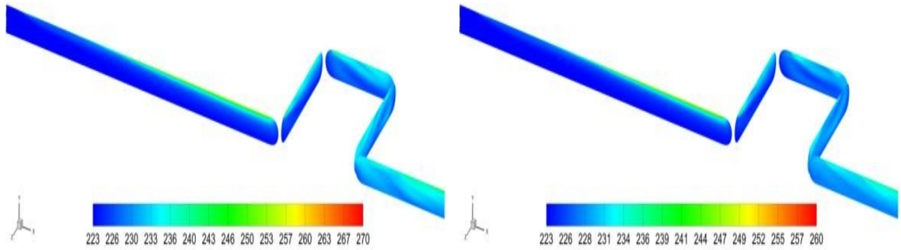

c) d)

Fig. 10. Temporal fluid temperature distribution across pipeline cross-sections along gravity.

In summary, during the pre-cooling process, temperature stratification also occurs in the fluid within the entire expansion bend pipe, with the inlet straight pipe segment being particularly evident. The reason for this is the same as that for temperature stratification in the fluid of the tank feed pipe. The density of the pre-cooling medium varies with temperature, and after heat exchange with the pipe, the fluid temperature rises and its density decreases, leading to the formation of stratification under the action of gravity and buoyancy. In the expansion bend segment, the disturbance caused by the bend mixes the fluid, and after multiple passages through the bend, the fluid temperature distribution in the outlet straight pipe segment becomes more uniform, and the heat exchange with the pipe wall is more balanced. Additionally, the turbulence within the bend disrupts the flow and temperature boundary layers to some extent, enhancing the heat exchange between the fluid and the pipe wall. Therefore, the pipe wall temperature at the bend decreases, and the temperature difference between the top and bottom of the pipe wall diminishes.

3 Conclusions

Through numerical simulation, this study primarily analyzed the distribution patterns of temperature and velocity fields in expanding elbow pipes under different process conditions and drew the following conclusions: During the pre-cooling and cold retention cycles, due to changes in the physical properties of the medium with temperature, and influenced by gravity and buoyancy, the fluid temperature and velocity inside the pipe tend to stratify in the direction of gravity. This results in temperature differences between the top and bottom of the pipe wall due to unequal heat exchange with the pipe wall. Typically, at the beginning of each pre-cooling stage, the temperature decrease rate at the bottom is faster than that at the top, but this situation reverses later. When the fluid flows through the expanding elbow pipe, the disturbance caused by the elbow disrupts the flow, leading to higher velocities on the inside of the bend compared to the outside, and lower temperatures on the inside than on the outside. This creates vortices that disrupt temperature stratification and the boundary layer, enhancing heat exchange with the pipe wall. Consequently, the temperature decrease at the top is more significant than at the bottom, with an accelerated temperature drop rate and a reduced temperature difference between the top and bottom. Simultaneously, this affects the fluid temperature and velocity in the downstream straight pipe segment. Compared to the inlet segment, the fluid temperature and velocity distribution in the outlet straight pipe segment are more balanced, indicating that the presence of the expanding elbow pipe can, to a certain extent, reduce the temperature difference between the top and bottom of the pipe and ensure pipeline safety.

Acknowledgments

This research was funded by National Key R&D Program of China, grant number. 2022YFC3070100; Young Elite Scientists Sponsorship Program by Beijing Association for Science and Technology, grant number. BYESS2023261; National Natural Science Foundation of China, grant number. 52304013; the Science and Technology Research Project of Pipechina, grant number. WZXGL202105; the Science and Technology Research Project of Pipechina, grant number. WZXGL202104; Science Foundation of China University of Petroleum, Beijing, grant number.2462023BJRC005 and the Science and Technology Research Project of Pipechina, grant number. CLZB202301.

References

1. Shukri T (2004) LNG technology selection. J. Hydrocarbon Engineering.Commun.,9(2): 71-72, 74, 76.
2. Castillo L, Dorao C A (2013) On the conceptual design of pre-cooling stage of LNG plants using propane or an ethane/propane mixture. J. Energy Conversion and Management.Commun.,65: 140-146.
3. Wu C, Liu J and Zhang J (2024) Transient thermal analysis on pre-cooling process of LNG cryogenic corrugated hose. J. Geoenergy Science and Engineering. Commun., 232: 212434.
4. Yuan K, Ji Y and Chung J N (2007) Cryogenic chilldown process under low flow rates. J. International Journal of Heat and Mass Transfer. Commun.,50(19-20): 4011-4022.
5. Yuan K, Ji Y and Chung J N (2009) Numerical modeling of cryogenic chilldown process in terrestrial gravity and microgravity. J. International Journal of Heat and Fluid Flow. Commun., 30(1): 44-53.
6. Wang L, Li Y and Zhao Z (2013) Transient thermal and pressurization performance of LO_2 tank during helium pressurization combined with outside aerodynamic heating. J. International Journal of Heat and Mass Transfer. Commun.,62: 263-271.
7. Ludwig C, Dreyer M E (2014) Investigations on thermodynamic phenomena of the active-pressurization process of a cryogenic propellant tank. J. Cryogenics. Commun.,2014, 63: 1-16.
8. In S, Jeong S and Kim H (2004) Investigation on liquid helium pressurization process using a heater in a liquid propellant rocket. J. Cryogenics. Commun.,44(6-8): 467-474.
9. Barsi S, Kassemi M (2008) Numerical and experimental comparisons of the self-pressurization behavior of an LH2 tank in normal gravity. J. Cryogenics. Commun., 48(3-4): 122-129.
10. Kassemi M, Kartuzova O (2016) Effect of interfacial turbulence and accommodation coefficient on CFD predictions of pressurization and pressure control in cryogenic storage tank. J. Cryogenics. Commun., 74: 138-153.